JOURNAL OF NANO- AND ELECTRONIC PHYSICS
Vol. **12** No 3, 03023(6pp) (2020)

ЖУРНАЛ НАНО- ТА ЕЛЕКТРОННОЇ ФІЗИКИ
Том **12** № 3, 03023(6cc) (2020)

Effect of Fe-incorporation on Structural and Optoelectronic Properties of Spin Coated *p/n* Type ZnO Thin Films

C. Zegadi[1,*], M. Adnane[2], D. Chaumont[3], A. Haichour[1], A. Hadj kaddour[4], Z. Lounis[4], D. Ghaffor[4]

[1] *Laboratoire de Micro et de Nanophysique (LaMiN), Ecole Nationale Polytechnique d'Oran Maurice AUDIN (ENPO-MA), BP 1523 El-Mnaouer, 31000 Oran, Algeria*
[2] *Laboratory of Electron Microscopy and Materials Sciences, University of Science and Technology of Oran, P.O. Box 1505, El-Mnaouer, 31000 Oran, Algeria*
[3] *Équipe NanoForm, Laboratoire ICB, Université de Bourgogne, 9, Ave Alain Savary, 21078 Dijon, France*
[4] *Laboratory of LABMAT, National Polytechnic School of Oran, ENP Oran- Maurice AUDIN, Oran, Algeria*

(Received 03 February 2020; revised manuscript received 15 June 2020; published online 25 June 2020)

This paper reports the effect of Fe incorporation on structural and electro-optical properties of ZnO thin films prepared by spin coating techniques. The Fe/Zn nominal volume ratio was 7 % in the solution. X-ray diffraction patterns of the films showed that doped incorporation leads to substantial changes in the structural characteristics of ZnO films. All the films have polycrystalline structure, with a preferential growth along the ZnO (002) plane. The crystallite size was calculated using a well-known Scherrer's formula and found to be in the range of 22-17 nm. The highest average optical transmittance value in the visible region was belonging to the Fe doped ZnO film. The results of the Raman scattering confirmed the observations of XRD and UV-Vis analysis techniques by the appearance of these occupancies at Zn^{+2} sites. These results are explained theoretically and are compared with those reported by other workers. The results of Hall measurement of ZnO and ZnO:Fe thin films reveal a high electron concentration around 1016 cm^{-3} and low mobility 2.6 cm^2/Vs. All as-grown samples show ambiguous carrier conductivity type (*p*-type and *n*-type) in the automatic Van der Pauw Hall measurement. A similar result has been observed in Li-doped ZnO and in As-doped ZnO films by other groups before. However, by characterizing our samples whit XPS, we have demonstrated that the ambiguous carrier type *n* in intended our ZnO films is not intrinsic behavior of the samples. It is due to the persistent photoconductivity effect in ZnO.

Keywords: ZnO films, Fe-doping, X-ray pattern, UV-Vis spectra, Raman scattering, *p*/*n*-type conductivity, XPS spectrum.

DOI: 10.21272/jnep.12(3).03023 PACS numbers: 61.05.cp, 51.50. + v, 07.60.Rd

1. INTRODUCTION

Fe-doped ZnO (ZnO:Fe) has attracted a great attention due to the possibility that it gives to expand the applications of ZnO in a wide variety of fields such as manufacturing of optical components, microelectronic devices and diluted magnetic semi-conductors [1-3]. Many techniques are used to develop ZnO and ZnO:Fe such as sputtering [4], chemical vapor deposition [5], sol-gel spin-coating and spray pyrolysis [6]. The sol-gel spin-coating method has been the scientific main interest over the last few years due to the low temperature used in the processing of materials. It is one of the most efficient methods for the preparation of nanostructured metal oxides and represents a relatively simple processing and a low cost alternative to the vacuum deposition techniques [7, 8]. Based on that, we have chosen the zinc oxide and Fe-doped zinc oxide as base materials deposited by the spin-coating process on glass substrates.

Indeed, they are relatively easy to be deposited and are among the most interesting materials from the point of view of properties compared to other materials [9, 10]. Therefore, to study their structural, optical and electrical properties, pure ZnO and ZnO:Fe thin films have been characterized by several techniques such as XRD data, UV-Vis spectra, Raman scattering, Hall effect measurements and XPS spectrum.

2. EXPERIMENTAL

2.1 Sol-gel Spin-coating Process

The deposition of undoped ZnO was performed using the sol-gel spin-coating method. A starting solution (0.1 mol/l) of zinc acetate dihydrate ($Zn(CH3COO)_2.2H_2O$; 29088.29; Normapur, France), dissolved in absolute ethanol (C_2H_5OH; 24103; Sigma Aldrich, Germany), was stirred (250 rotations per minute) at 90 °C for 3 h in order to yield a transparent, homogeneous and stable solution. Glass substrates (Super Premium Microscope Slides; VWR International; 75×25×1 mm^3) were cleaned in an ultrasonic bath for 10 min and rinsed by ethanol. The respective sols were spin coated on glass substrates at 3000 rpm. After each deposition stage, the covered substrates were heated in a laboratory oven at 120 °C for 5 min in air in order to remove the volatile materials. The coating procedure was repeated five times before applying a post-heat treatment to the coated glass substrates at 550 °C for 2 h.

Regarding the deposition of Fe-doped ZnO, it was performed using the same process: except that to the starting solution used for undoped ZnO, iron (III) chloride hexahydrate ($FeCl_3.6H_2O$; 44944; Fluka, France) was added after 20 min, the time needed to have a clear and homogenous solution.

*chawki.zegadi@enp-oran.dz

2.2 Characterization

Using pure ZnO and ZnO:Fe samples, with the help of the Siemens D500 X-Ray Diffractometer (XRD) at room temperature, the diffractometer reflections were produced by scanning the sample through a range of 2θ angles swapped between 20° and 70° with Cu-KL_α radiation and a scanning speed of 0.05 °/min. The incident wavelength was 1.54056 Å. The optical transmittance measurements of the films were performed using a UV-Visible spectrophotometer (Shimadzu 1200) and the optical band gap energy was calculated. The optical transmittance was also measured with an integrating sphere in a wavelength range of 190-900 nm. The Raman spectroscopy technique was employed to study the crystalline quality and structural disorders, using a microscopic confocal Raman spectrometer (Renishaw RM1000).The electrical resistivity measurements of the films were carried out using the ECOPIA HMS 3000 Hall effect measurement system at room temperature (T = 300 K) and a magnetic field of 0.58 T. The valence states of the elements in ZnO and ZnO:Fe were determined by VG Multilab 2000 X-ray photoelectron spectroscopy (XPS).

3. RESULTS AND DISCUSSION

3.1 X-ray Diffraction (XRD)

Fig. 1 shows the XRD patterns of undoped ZnO and Fe-doped ZnO films. For all samples, the peak position agrees well with the reflections of hexagonal wurtzite type structure of polycrystalline ZnO (JCPDS Card No. 36-1451). No parasitic phase (impurity peak) is observed in the detection limit of the apparatus, indicating a high purity of the samples. The diffraction peaks arise at (002) 34.22° and (103) 62.54° for undoped and (002) 34.046°, (110) 56.203° and (103) 62.4345° for Fe-doped ZnO. The orientation of crystallites in undoped films (two peaks) is better than the one in doped films (three orientations). We observed in all patterns of ZnO thin films a high diffraction intensity for the peak (002). This result implies that the film exhibits preferential orientation along the (002) plane direction (c-axis). Furthermore, up on increasing the Fe dopant concentration, the intensity of (002) peak increases. The peak position of the (002) plane was shifted to the smaller diffraction angles. Because of the almost similar ionic radius of the dopant ions Fe^{+3} and Zn^{2+} ions comparing with the dopant ions substituted for Zn^{2+} ions. Similar shifts that were in agreement with those have also been observed by Tsay et al. [11].

The lattice spacing was calculated from the following Bragg's formula [11]:

$$2d_{hkl}\sin\theta_{hkl} = n\cdot\lambda, \quad (1)$$

where d_{hkl} is the lattice spacing, θ_{hkl} is the angle of incidence or Bragg diffraction, λ is the wavelength of the radiation and n is the diffraction order (n = 1, 2, ...).

From the ZnO (002) diffraction peak the lattice constant (c) is expressed as follows:

$$C = 2d_{002} = \lambda / \sin\theta_{002}. \quad (2)$$

The lattice spacing (d_{hkl}), I/I_{High} ratio where I is the measured relative intensity of a plane (hkl), I_{High} is the highest intensity of the plane (hkl) taken from the data, angle of diffraction (2θ) at the phases identified along with (hkl) planes of the films and the lattice constant (c) are given below in Table 1.

Table 1 – 2θ, d_{hkl} and I/I_{High} values of undoped and Fe-doped ZnO films

Film	(hkl)	2θ(°)	d (Å)	c (Å)	$I/I_{High}\times$ 100
ZnO	(002)	34.22	2.61	5.22	100.0
	(103)	62.54	1.48	/	12.98
ZnO:Fe	(002)	34.05	2.61	5.22	100.0
	(110)	56.20	1.54	/	3.39
	(103)	62.43	1.49	/	2.68

The crystallite size of the thin films was determined using the peak (002) by Scherrer's formula [11]:

$$D = K\lambda / \beta\cos\theta_{(hkl)}, \quad (3)$$

where D is the crystallite size, λ = 0.154056 nm means the wavelength of CuKα1 radiation and β is the full-width half maximum (FWHM) of the Bragg peak observed at Bragg angle θ (rad), K = 0.89. The values of D obtained indicate, that the crystallites decrease with the incorporation of Fe, which is in agreement with literature [12]. It is 23 nm for the 7 %-Fe-doped and 41 nm for the undoped ZnO.

As a result, the incorporation of Fe in the lattice of ZnO has been demonstrated through the modification of the lattice spacing b displacing the diffraction peak (002), associating the scanning rate, and applying an influence on the crystallite size, so the Fe-doped ZnO films can reduce the average crystallite size. Furthermore, the XRD clearly showed that the doping displayed an important role for improving the structure of the ZnO films.

Table 2 – Structural parameters of pure and Fe-doped ZnO films

Film	D(nm)	β(°)	$\delta\times10^{-6}$ (line^2/Å^2)	$\varepsilon\times10^{-6}$	$\rho\times10^{-6}$ (line^2/Å^2)
ZnO	41	0.174	127.47	7667.25	988.62
ZnO:Fe	27	0.296	60.65	5332.23	568.66

The dislocation density (ρ) is defined as the length of dislocation lines per unit volume of the crystal. It has two components: the first is due to the size (δ) which has been calculated by the formula [12]:

$$\delta = 3\times n / D^2 \quad (4)$$

and another one is due to the lattice strain (ε) whose value can be calculated using Stokes-Wilson equation [13]:

$$\varepsilon = \beta / 4\tan\theta. \quad (5)$$

The resultant dislocation density was estimated according to the following relation:

$$\rho = (\delta\times\varepsilon)^{1/2}. \quad (6)$$

The values of the dislocation density (imperfection of crystallites) are given in Table 2, where the incorpora-

tion of Fe reveals clearly the deterioration in the crystallinity. As a result, the layers are under compressive stress, so that it compresses and relaxes afterwards.

The crystallization levels of the as-grown films are of high quality because of their larger D, their smaller FWHM and their smaller dislocation density.

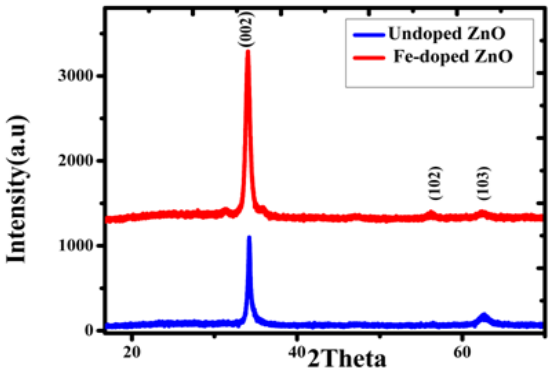

Fig. 1 – XRD patterns of undoped and Fe-doped ZnO films

3.2 Optical Transmission

The transmittance spectra of undoped and Fe-doped ZnO films are shown in Fig. 2. It is found that the transmittance is above 80 %. Based on that, the optical band gap E_g was obtained by extrapolating the linear portion of the plot $(\alpha h\nu)^2$ versus $(h\nu)$ to $\alpha = 0$ according to the following equation:

$$\alpha = A\left(h\nu - E_g\right)^n, \qquad (7)$$

where $h\nu$ is the photon energy, E_g is the band gap, A is the edge parameter and $n = 1/2$ for direct gap material. The optical band gaps E_g of undoped and Fe-doped ZnO films are illustrated in Fig. 3 and Fig. 4, respectively. While the band gap is 3.20 eV for the undoped ZnO film, it rises to 3.23 eV for the one with Fe-doped ZnO. The change in the optical band gap of the Fe-doped ZnO film was bound up with the valence state of Fe ions. If the (Fe^{3+}) ions have entered the lattice sites, previously occupied by Zn ions, they would provide additional free carriers that cause the Fermi level to move into the conduction band, allowing the band-gap of ZnO:Fe to increase.

Table 3 – Optical parameters of pure and Fe-doped ZnO films

Film	T_{ave} (%)	E_g (eV)	E_u (meV)
ZnO	87.5	3.198	629.92
ZnO:Fe	83.6	3.23	276.64

It is also assumed that the absorption coefficient near the band edge shows an exponential dependence on the photon energy. This dependence is illustrated as following [12]:

$$\alpha = \alpha_0 \exp\left(E / E_U\right), \qquad (8)$$

where E is the photon energy, α_0 is the constant and E_U is the Urbach energy which refers to the width of the exponential absorption edge. Inset plots of Fig. 3 and Fig. 4 show the variation of lnα vs. photon energy for the films. This behavior corresponds primarily to the optical transitions between the occupied states in the valence band tail to the unoccupied states at the conduction band edge. The E_U value was calculated from the slope of Fig. 3 and Fig. 4 using the relationship:

$$E_U = \left[\left(d\left(\ln\alpha\right)\right) / d\left(h\nu\right)\right]^{-1}. \qquad (9)$$

The values of E_U obtained from this figure are given in Table 3. The E_U values change inversely with the optical band gaps of the films. A similar result of E_U has been observed by other groups of different doped ZnO films prepared by the sol-gel process [12, 14].

3.3 Raman Scattering

Raman spectroscopy is considered to be the most powerful and no destructive technique to study the crystalline quality, the structural disorder and the defects in the host lattice [15]. The Raman scattering spectrum of undoped ZnO is presented in Fig. 5. The second-order vibration mode and A1 (TO) modes have been observed at 781 cm^{-1} and 946 cm^{-1} frequencies, respectively, the phonon frequency of E2 (high) at 989 cm^{-1} and E1 (LO) modes at 1096 cm^{-1}, which involves the motion of oxygen and is characteristic of wurtzite structure compared with those of undoped ZnO.

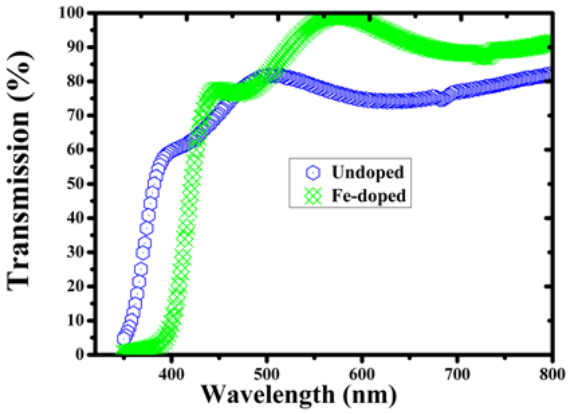

Fig. 2 – Transmittance spectra of undoped and doped ZnO films

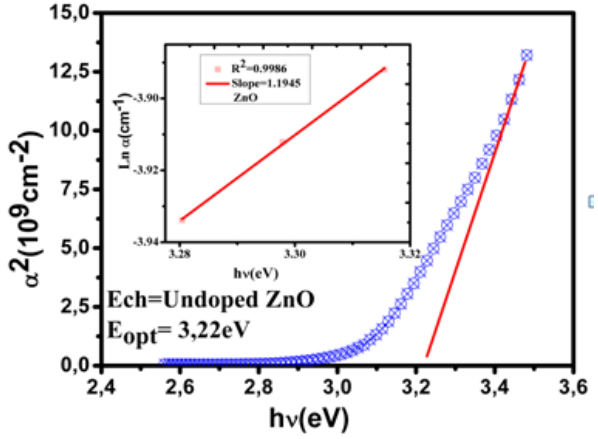

Fig. 3 – The plots of $(ahv)^2$ versus hv and Urbach plots (inset plots) of undoped ZnO films

The Fe-doped ZnO (Fig. 6) has the classical Raman modes at 774, 946, 990, and 1092 cm^{-1} and an additional mode at 1221 cm^{-1}. This additional mode is related to intrinsic host-lattice defects or due to Fe^{+3} occupation at Zn^{+2} sites according Zhang et al. [16] who observed the vibration mode at 1288 cm^{-1} in Fe, Sb, Al, Ga, and Li-doped ZnO films and proposed that this additional mode is related to intrinsic host-lattice defects. In our experiment, the additional mode does not appear before or after doping, which allows us to say that our films have less intrinsic defects [17]. These observations are in good agreement with the data of DRX and UV-Vis.

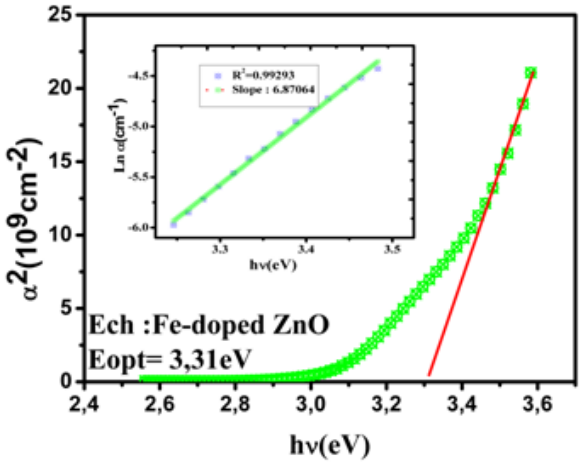

Fig. 4 – The plots of $(ahv)^2$ versus hv and Urbach plots (inset plots) of Fe-doped ZnO films

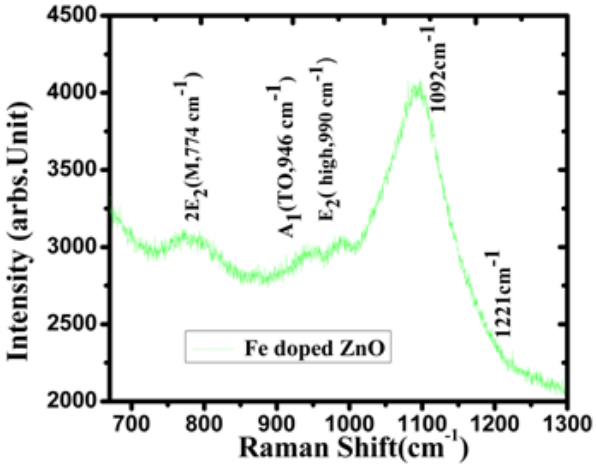

Fig. 5 – Room-temperature Raman spectra of ZnO:Fe

3.4 The Hall Effect Measurement

The Hall Effect measurement system is useful for determining various material parameters. The primary of these parameters is the Hall voltage (V_H), since the carrier mobility, the carrier concentration (n), the Hall coefficient (R_H), the resistivity and the carrier conductivity type (N or P) are all derived from Hall voltage [18, 19]. In this experience, the Van der Pauw Hall measurement was performed in a homemade automatic four-probe Hall measurement system (referring to Fig. 7).

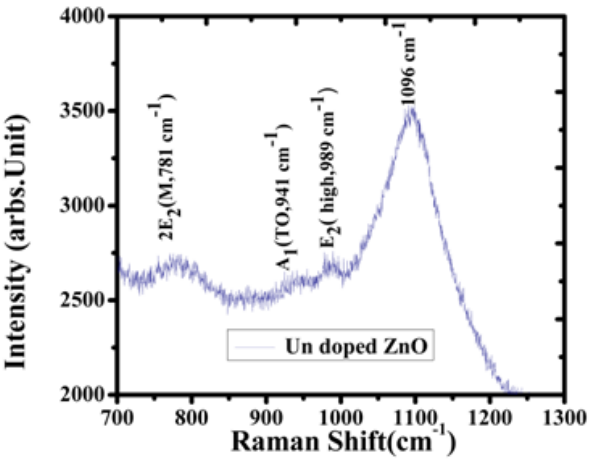

Fig. 6 – Room-temperature Raman spectra of ZnO

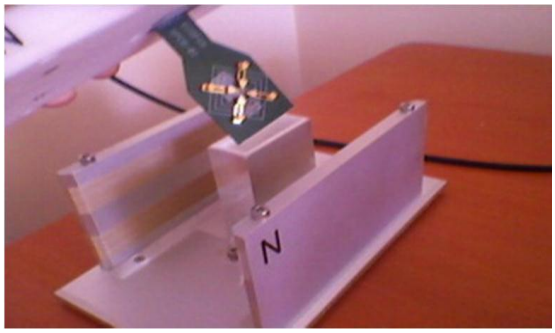

Fig. 7 – Hall measurement apparatus of undoped ZnO and Fe-doped ZnO. The films are kept by four Au probes as signed by the arrow

Table 4 – Data of the Van der Pauw Hall measurement

Films	ZnO	ZnO:Fe
Carrier concentration (cm^{-3})	4.29×10^{17}	1.073×10^{16}
Mobility (cm^2/Vs)	2.69×10^{0}	1.06×10^{1}
Conductivity (μS/m)	1.85×10^{-7}	1.83×10^{-7}
Resistivity (Ω-cm)	5.40×10^{8}	5.48×10^{7}
Type	*p*/*n*	*p*/*n*

Van der Pauw Hall measurement was conducted on 5 mm × 5 mm samples with a dc current $I = 100$ nA and a magnetic field $B = 0.58$ T. The as-grown ZnO film exhibited n-type conductivity as cited previously [1-3]. All of the as-grown samples by spin-coating process exhibited carrier p/n-type conductivity with a decrease in the electron concentration from 4.29×1017 cm^{-3} (ZnO) to 1.073×1016 cm^{-3} (ZnO:Fe). Similar results have been observed in Li- and Ga-doped ZnO by other groups before [16]. The results of the samples are given in Table 4.

Therefore, to further determine the reason behind the appearance of the carrier p-type in these samples, the XPS measurement was performed for our samples, traced in detail to confirm this carrier p-type conductivity. The analysis by XPS for Fe-doped ZnO and pure ZnO films gives no nitrogen peak and shows an oxygen deficiency. This is probably due to the low air absorption of our samples at the level of pre-drying which takes place in an ambient air. This result allows us to confirm the cause of the carrier p/n-type conductivity in our ZnO films.

3.5 The Van der Pauw

The bonding element of the Fe-doped and pure ZnO films was examined by XPS as shown in Fig. 8. This figure shows the result of XPS spectra of the ZnO and FZO films with full region scanning from 0 to 1100 eV. Comparing the FZO film with the ZnO film, we can note that the intensity of the major binding energy peak had slightly decreased. The high-resolution scanning information provided in Fig. 8 is related respectively to the separate analysis of 3 elements: O, Zn and Fe. These elements were detected in the spectrum, and Auger peaks such as Zn LMM and O KVV were also observed from the Fe-doped bulk [20].

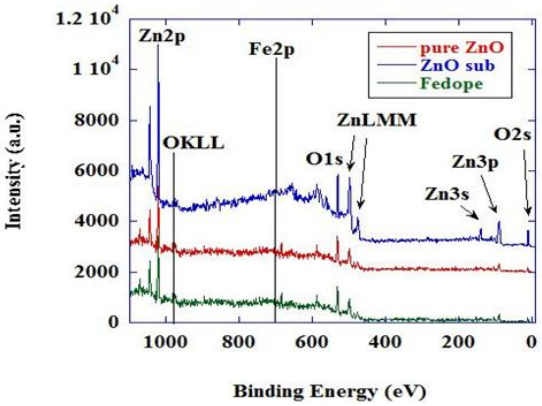

Fig. 8 – The XPS survey spectrum of FZO and ZnO thin films

After the characterization of our Fe-doped ZnO and undoped ZnO samples by XPS, we could determine the type of our films by no nitrogen peak. This allows us to say that our type is not *p*/*n*, but it is *n* conductivity.

In summary, the Van der Pauw Hall measurement has been performed on the intended undoped ZnO film, Fe-doped ZnO film and undoped ZnO film grown by using a spin coating process. All of the as-grown samples show an ambiguous carrier *p*-type or *n*-type conductivity. The electron concentration decreases with the doping impurity and the mobility becomes smaller. By characterizing our samples with XPS, we have demonstrated that the ambiguous carrier type *n* in our intended ZnO films is not an intrinsic behavior of the samples. We think it is due to the persistent photoconductivity effect in ZnO. This effect strongly affects the determination of the carrier conductivity type in highly resistive intended ZnO samples for *p*-type conductivity. We suggest that the study of the self-compensating effect and the deep-energy impurity states would be very important to overcome the *p*-doping problem of ZnO.

4. CONCLUSIONS

Undoped zinc oxide and Fe-doped zinc oxide thin films have been prepared by spin coating process in an ambient atmosphere. The advantages of this technique come from the simplicity of the sol-gel process, its short duration, and the auxiliary materials availability. We set up a mechanism to control and operate the parameters of this technique, which helped us to obtain the structures with a high efficiency. The XRD analysis showed us that the structure was hexagonal for all the samples with decrease in the crystallite size of the Fe-doped ZnO particles. The undoped ZnO and Fe-doped ZnO films reveal a high visible transmittance (> 80 %). The optical band gap was (3.27 eV) for undoped and (3.28 eV) for Fe-doped. The Urbach energy values of these films have been determined and Raman spectrum has been traced to study the crystalline quality and structural disorder of the films. The results of Raman spectra are in good agreement with the data of XRD and UV-Vis. The Van der Pauw Hall effect measurement has revealed one kind of *p*-type and *n*-type conductivity, a very high electron concentration around 1.073×10^{16} cm^{-3} and a low mobility around 2.69 cm^2/Vs. Using a XPS measurement, we have demonstrated that the ambiguous carrier type *n* in our intended ZnO films is not an intrinsic behavior of our samples. We have explained that the appearance of *p*-type conductivity in our ZnO films is due to the persistent photoconductivity effect in ZnO.

ACKNOWLEDGEMENTS

The authors would like to thank the Japan International Cooperation Agency (JICA) and the generous assistance of Dr. Y. Harada from National Institute for Materials Science, Namiki, and Tsukuba, Japan for the analysis made by XPS and K. Tsubouchi from University of Tokyo for their support and correction.

REFERENCES

1. Y.K. Mishra, R. Adelung, *Mater. Today* **21** No6, 635 (2018).
2. F. Pan, C. Song, X.J. Liu, Y.C. Yang, F. Zeng, *Mater. Sci. Eng. R Rep.* **62** No 1, 1 (2008).
3. N.O. Korsunska, L.V. Borkovska, B.M. Bulakh, L.Yu. Khomenkova, V.I. Kushnirenko, I.V. Markevich, *J. Lumin* **102-103**, 733 (2003).
4. J. Rodríguez-Báez, A. Maldonado, G. Torres-Delgado, R. Castanedo-Pérez, M. de la L.Olvera, *Mater. Lett* **60** No 13-14, 1594 (2006).
5. M. Jin,J, Feng, Z. De-heng, M, Hong-lei, L. Shu-ying, *Thin Solid Films* **375** No2, 98 (1999).
6. W. Tang, D.C. Cameron, *Thin Solid Films* **238** No 1, 38 (1994).
7. A.B. Djurišić, A.M.C. Ng, X.Y. Chen, *Prog. Quant. Electron.* **34** No 4, 191 (2010).
8. P. Sharma, A. Gupta, K. Rao, *Nature Mater.* **2**, 673 (2003).
9. M. Zerdali, S. Hamzaoui, F.H. Teherani, D.J. Rogers, *Mater Lett* **60** No 4, 504 (2006).
10. Y. Bakhaa, K.M. Bendimerad, S. Hamzaoui, *Eur. Phys. J. Appl. Phys* **55** No 3, 30103 (2011).
11. C.Y. Tsay, H.C. Cheng, Y.T. Tung, W.H. Tuan, C.K. Lin, *Thin Solid Films* **517** No 3, 1032 (2008).
12. S. Ilican, Y. Caglar, M. Calgar, B. Demirsi, *J. Optoelectron. Adv. M* **10** No 10, 2592 (2008).
13. M.A. Hassan, *IJP* **10** No 18, 17 (2012).
14. F. Yakuphanoglu, S. Ilican, M. Caglar, Y. Caglar, *J. Optoelectron Adv. M.* **9** No 7, 2180 (2007).
15. E. Senthilkumar, S. Venkatesh, M.S. Ramachandra Rao, *Appl. Phys. Lett.* **96** No 23, 232504 (2010).
16. C. Zhang, *J. Phys. Chem. Solids,* **71** No 3, 364 (2010).
17. M. Saeed Akhtar, M. Azad Malik, Y.G. Alghamdi, K.S. Ahmad, S. Riaz, S. Naseem, *Mat. Sci. Semicond. Proc.* **39**, 283 (2015).
18. P. Kathirvel, D. Manoharan, S.M. Mohan, S. Kumar, *JOBM* **1** No 1, 25 (2009).
19. S. Venkatachalam, R.T. Rajendrakumar, D. Mangalaraj, Sa.K. Narayandass, K. Kim, J. Yi, *Solid State Electron.* **48** No 12, 2219 (2004).
20. Y. Zhang, L. Wu, H. Li, J. Xu, L. Han, B. Wang, Z. Tuo, E. Xie, *J. Alloy. Compd.* **473** No 1-2, 319 (2009).

Вплив додавання Fe на структурні та оптоелектронні властивості тонких плівок ZnO *p*/*n* типу, нанесених методом центрифугування

C. Zegadi[1], M. Adnane[2], D. Chaumont[3], A. Haichour[1], A. Hadj kaddour[4], Z. Lounis[4], D. Ghaffor[4]

[1] *Laboratoire de Micro et de Nanophysique (LaMiN), Ecole Nationale Polytechnique d'Oran Maurice AUDIN (ENPO-MA), BP 1523 El-Mnaouer, 31000 Oran, Algeria*
[2] *Laboratory of Electron Microscopy and Materials Sciences, University of Science and Technology of Oran, P.O. Box 1505, El-Mnaouer, 31000 Oran, Algeria*
[3] *Équipe NanoForm, Laboratoire ICB, Université de Bourgogne, 9, Ave Alain Savary, 21078 Dijon, France*
[4] *Laboratory of LABMAT, National Polytechnic School of Oran, ENP Oran- Maurice AUDIN, Oran, Algeria*

У роботі повідомляється про вплив включення Fe на структурні та оптоелектронні властивості тонких плівок ZnO, отриманих методом центрифугування. Номінальне співвідношення Fe/Zn у розчині становило 7 %. Рентгенограми плівок показали, що леговане включення призводить до істотних змін структурних характеристик плівок ZnO. Усі плівки мають полікристалічну структуру з переважним зростанням вздовж площини (002) плівки ZnO. Розмір кристалітів був розрахований за відомою формулою Шеррера і виявився в діапазоні 22-17 нм. Найбільше середнє значення оптичного пропускання у видимій області спектру належало плівці ZnO, легованій Fe. Результати Раманівського розсіювання підтвердили спостереження методів XRD та УФ-спектроскопії появою цих місць на ділянках Zn^{+2}. Ці результати пояснюються теоретично і порівнюються з тими, про які повідомляється іншими дослідниками. Результати Холівських вимірювань тонких плівок ZnO та ZnO:Fe виявляють високу концентрацію електронів приблизно 1016 $см^{-3}$ та їх низьку рухливість 2.6 $см^2/Вс$. Усі вирощені зразки демонструють неоднозначний тип провідності носіїв (*p*- або *n*-тип) в автоматичних Холівських вимірюваннях Ван-дер Поу. Аналогічний результат спостерігався раніше іншими групами у плівках ZnO, легованих Li та As. Однак, охарактеризувавши зразки рентгено-електронною спектроскопією (XPS), ми продемонстрували, що неоднозначний *n*-тип носіїв у наших плівках ZnO не є внутрішньою поведінкою зразків, а обумовлений стійким ефектом фотопровідності в ZnO.

Ключові слова: Плівки ZnO, Fe-легування, Рентгенограма, Ультрафіолетова та видима області спектру, Раманівське (комбінаційне) розсіювання, Електропровідність типу *p*/*n*, Спектр XPS.